OPEN ACCESS
CellPress

Cell Reports
Article

Control of Disease Tolerance to Malaria by Nitric Oxide and Carbon Monoxide

Viktória Jeney,[1,4,6] Susana Ramos,[1,6] Marie-Louise Bergman,[1] Ingo Bechmann,[2] Jasmin Tischer,[2] Ana Ferreira,[1,5] Virginia Oliveira-Marques,[1] Chris J. Janse,[3] Sofia Rebelo,[1] Silvia Cardoso,[1] and Miguel P. Soares[1,*]

[1]Instituto Gulbenkian de Ciência, 2780-156 Oeiras, Portugal
[2]Faculty of Medicine, Institute of Anatomy, 04103 Leipzig, Germany
[3]Leiden Malaria Research Group, Department of Parasitology, Center of Infectious Diseases, Leiden University Medical Center, 2300 RC Leiden, the Netherlands
[4]Present address: Department of Medicine, University of Debrecen, Nagyerdei körút 98., Debrecen 4032, Hungary
[5]Present address: Faculdade de Ciências Sociais e Humanas da Universidade Nova de Lisboa, Avenida de Berna, 26-C/1069-061 Lisbon, Portugal
[6]Co-first author
*Correspondence: mpsoares@igc.gulbenkian.pt
http://dx.doi.org/10.1016/j.celrep.2014.05.054

SUMMARY

Nitric oxide (NO) and carbon monoxide (CO) are gasotransmitters that suppress the development of severe forms of malaria associated with *Plasmodium* infection. Here, we addressed the mechanism underlying their protective effect against experimental cerebral malaria (ECM), a severe form of malaria that develops in *Plasmodium*-infected mice, which resembles, in many aspects, human cerebral malaria (CM). NO suppresses the pathogenesis of ECM via a mechanism involving (1) the transcription factor nuclear factor erythroid 2-related factor 2 (NRF-2), (2) induction of heme oxygenase-1 (HO-1), and (3) CO production via heme catabolism by HO-1. The protection afforded by NO is associated with inhibition of $CD4^+$ T helper (T_H) and $CD8^+$ cytotoxic (T_C) T cell activation in response to *Plasmodium* infection via a mechanism involving HO-1 and CO. The protective effect of NO and CO is not associated with modulation of host pathogen load, suggesting that these gasotransmitters establish a crosstalk-conferring disease tolerance to *Plasmodium* infection.

INTRODUCTION

Plasmodium infection can lead to the development of cerebral malaria (CM) (Mishra and Newton, 2009), an often-lethal neurovascular syndrome, triggered by maladaptive host immunity (Miller et al., 2013) and the sequestration of *Plasmodium*-infected red blood cells (RBCs) in the brain microvasculature (Taylor et al., 2004). These pathologic events lead to the disruption of the blood brain barrier (BBB), brain edema, and coma, the hallmarks of CM (Mishra and Newton, 2009).

As for other clinical manifestations of malaria, CM arises exclusively during the blood stage of *Plasmodium* infection (Miller et al., 2013), associated with hemolysis and hence with the generation of cell-free hemoglobin (Hb) (Andrade et al., 2010; Ferreira et al., 2008; Francis et al., 1997). When oxidized into (ferric) methemoglobin (MetHb), extracellular Hb releases its prosthetic heme groups (Balla et al., 1993; Bunn and Jandl, 1968; Gozzelino et al., 2010). Free heme is proinflammatory (Figueiredo et al., 2007), cytotoxic (Balla et al., 1993; Gozzelino et al., 2010; Seixas et al., 2009), and vasoactive (Belcher et al., 2014), thus promoting the pathogenesis of experimental cerebral malaria (ECM) (Ferreira et al., 2008, 2011; Pamplona et al., 2007), a neurovascular syndrome that develops in *Plasmodium berghei* ANKA (PbA)-infected mice and that resembles in many aspects human CM that develops in response to *P. falciparum* infection (Mishra and Newton, 2009).

The pathogenesis of ECM is fueled by the activation of $CD4^+$ T helper (T_H) and $CD8^+$ cytotoxic T (T_C) cells (Belnoue et al., 2002, 2008; Nitcheu et al., 2003; Villegas-Mendez et al., 2012) that migrate into the brain microvasculature, via a mechanism involving the expression of the chemokines CXCL9, CXCL-10/IP10, and their cognate receptor CXCR3 (Campanella et al., 2008; Miu et al., 2008). Interaction of activated T_H and T_C with microvascular endothelial cells in the brain compromises BBB integrity via a mechanism involving the expression of Perforin (Prf) (Nitcheu et al., 2003) and granzyme B (GzmB) (Haque et al., 2011) by activated T_C cells. This cytotoxic effect synergizes locally with free heme to trigger ECM (Ferreira et al., 2008, 2011; Gozzelino et al., 2010).

Mammals have a variety of protective mechanisms restraining the deleterious effects of heme, which converge at the level of heme catabolism by heme oxygenase-1 (HO-1) (encoded by the *HMOX1* gene), generating equimolar amounts of carbon monoxide (CO), labile Fe, and biliverdin (Tenhunen et al., 1968). Induction of HO-1 expression in response to *Plasmodium* infection suppresses the pathogenesis of ECM (Ferreira et al., 2008, 2011; Pamplona et al., 2007) as well as the pathogenesis of noncerebral forms of severe malaria in mice (Ferreira et al., 2008; Seixas et al., 2009). This protective effect is not associated with modulation of host pathogen load, thus suggesting that

HO-1 does not regulate host resistance to *Plasmodium* infection. Instead, HO-1 limits tissue damage imposed to the host during infection, suggesting that it confers disease tolerance (Ayres and Schneider, 2012; Medzhitov et al., 2012; Schneider and Ayres, 2008) to *Plasmodium* infection. In contrast to resistance to infection, disease tolerance limits disease severity (Schneider, 2011) via a mechanism that does not necessarily impact on the host pathogen load (Medzhitov et al., 2012; Schneider and Ayres, 2008). In keeping with this notion, the survival advantage afforded by sickle Hb against malaria acts via a mechanism that involves the induction of HO-1, conferring disease tolerance to *Plasmodium* infection (Ferreira et al., 2011). Moreover, polymorphisms in the *HMOX1* gene correlate with incidence of severe forms of malaria in human populations (Andrade et al., 2010), including CM (Walther et al., 2012). Overall, this argues strongly for the involvement of HO-1 in the regulation of disease severity in response to *Plasmodium* infection in mice as well as in humans.

CO contributes critically to the protective effect of HO-1 against ECM (Ferreira et al., 2008, 2011; Pamplona et al., 2007). This salutary effect relies on the avid binding of CO to the prosthetic heme groups of cell-free Hb and the formation of a not readily oxidized carboxyhemoglobin (CO-Hb) complex (Hebbel et al., 1988; Pamplona et al., 2007). This antioxidant effect restrains the pathogenic effects of cell-free Hb (Silva et al., 2009) and prevents the proinflammatory (Figueiredo et al., 2007) and cytotoxic (Gozzelino et al., 2010; Larsen et al., 2010; Seixas et al., 2009) effects associated with heme release from Hb, from partaking in the pathogenesis of ECM.

Cell-free Hb also contributes to pathogenesis of severe forms of malaria via nitric oxide (NO) scavenging, reducing NO bioavailability (Rother et al., 2005; Gramaglia et al., 2006) and promoting brain microvascular constriction associated with the pathogenesis of ECM (Cabrales et al., 2011; Gramaglia et al., 2006; Ong et al., 2013). That NO regulates the pathogenesis of severe forms of malaria is supported by the association of several polymorphisms in the genes encoding the nitric oxide synthase (NOS) isoforms 1 (Dhangadamajhi et al., 2009), 2 (Hobbs et al., 2002; Trovoada et al., 2014), and 3 (Dhangadamajhi et al., 2010) with malaria severity in human populations. Moreover, there is also a direct correlation between the levels of NO in plasma and the incidence of severe malaria in human populations (Anstey et al., 1996; Trovoada et al., 2014). Based on these observations, pharmacologic application of NO has been proposed as a supportive therapy for life-threatening complications of malaria (Hawkes et al., 2011; Yeo et al., 2013).

Here, we report that the protective effect of NO against ECM acts via a mechanism in which NO induces the expression of HO-1 through activation of the nuclear factor erythroid (NF-E) 2-related factor 2 (Nrf2), a member of the Cap 'n' Collar basic leucine zipper family of transcription factors (Itoh et al., 1999) that regulates adaptive cellular responses to oxidative stress (Itoh et al., 1997; Kensler et al., 2007; Suzuki et al., 2013). CO produced via heme catabolism by HO-1 mediates the protective effects of NO against ECM. NO and CO do not interfere with host pathogen burden, suggesting that these gasotransmitters confer disease tolerance to *Plasmodium* infection.

RESULTS

NO Confers Disease Tolerance to *Plasmodium* Infection

C57BL/6 mice succumbed to ECM when inoculated with RBCs infected with a transgenic *Pb*A-expressing GFP under the control of the EEF1α promoter; i.e., PbA$^{EEF1\alpha\text{-}GFP}$ infection (Figure 1A). Administration of the NO donor dipropylenetriamine NONOate (DPTA-NO) suppressed the onset of ECM (Cabrales et al., 2011; Gramaglia et al., 2006), with maximal protection at DPTA-NO administration starting 1–3 days before infection and twice daily thereafter for 7 days (Figure 1A). This protective effect was lost when DPTA-NO administration was started 1–3 days after infection (Figure 1A). When used at a protective dosage/schedule, DPTA-NO prevented brain microvascular congestion (Figure 1B), BBB disruption (Figure 1B), and brain edema (Figure 1C); i.e., the hallmarks of ECM. This protective effect was lost when DPTA-NO was administered 3 days after infection, as assessed for brain edema (Figure 1C).

DPTA-NO administration did not modulate parasitemia (i.e., percentage of circulating RBCs containing PbA$^{EEF1\alpha\text{-}GFP}$ parasites [Figure 1D]), while reducing parasite accumulation in the brain versus vehicle-treated controls, as assessed by quantitative real-time RT-PCR (Figure 1E). We asked whether NO reduces the sequestration of mature schizonts in the brain, using a transgenic PbA strain expressing a GFP/Luciferase fusion protein in mature schizonts, under the control of the AMA1 promoter; i.e., PbA$^{AMA1\text{-}GFP/LUC}$. NO had no impact on parasitemia, as quantified by the detection of *Plasmodium* DNA in circulating RBCs (Figure S1A), morphological detection of parasites in blood smears (Figure S1B), or percentage of circulating RBCs containing mature PbA$^{AMA1\text{-}GFP/LUC}$ schizonts, as detected by GFP (Figure S1C) or by luciferase (Figures 1F and 1G) expression. NO reduced schizont sequestration in the brain, spleen, and heart while increasing sequestration in the lung versus vehicle-treated controls, as quantified by luciferase activity (Figures 1H, S1D–S1G, and S1K). Sequestration was not affected in liver, kidney, and fat (Figures S1H–S1K). This suggests that whereas NO does not interfere with parasitemia, it reduces parasite biomass in the brain, an effect that should contribute to suppressing the pathogenesis of ECM (Miller et al., 2013).

DPTA-NO inhibited the accumulation of T_H and T_C cells in the brain of PbA$^{EEF1\alpha\text{-}GFP}$-infected mice versus control-infected mice receiving vehicle, as assessed by quantitative real-time RT-PCR for *Cd3e* (T cells), *Cd4* (T_H cells), and *Cd8a* (T_C cells) mRNA expression (Figure 1I). This immunomodulatory effect should also contribute to suppressing the pathogenesis of ECM (Belnoue et al., 2002, 2008; Nitcheu et al., 2003; Villegas-Mendez et al., 2012).

The Protective Effect of NO Acts via a Mechanism Involving the Induction of HO-1 Expression

DPTA-NO administration induced the expression of *Hmox1* mRNA in C57BL/6 mice, as quantified in different organs by quantitative real-time RT-PCR (Figure 2A) (Motterlini et al., 1996). This was associated with induction of HO enzymatic activity, as assessed by the relative rate of biliverdin/bilirubin generation (Figure 2B) as well as by CO

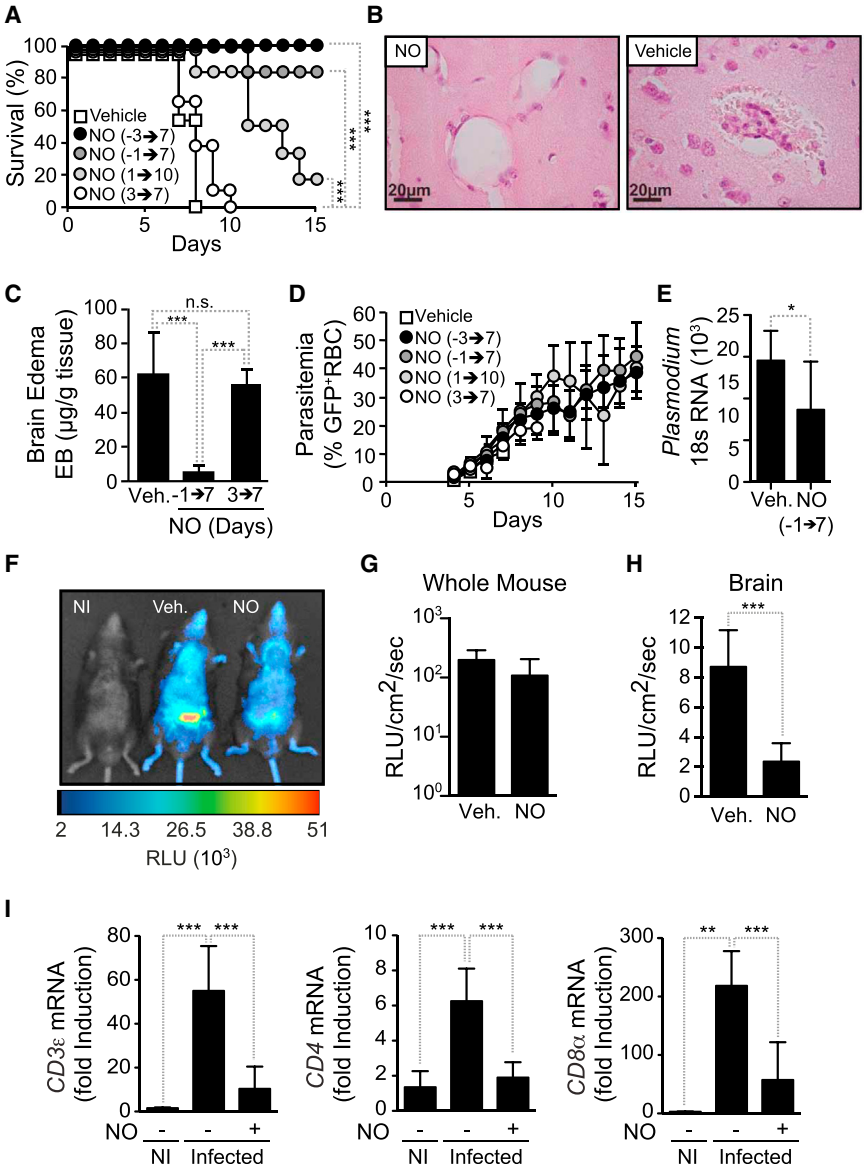

Figure 1. NO Suppresses ECM and Confers Disease Tolerance to *Plasmodium* Infection

(A) Survival of PbA$^{EEF1\alpha\text{-}GFP}$-infected C57BL/6 mice receiving DPTA-NO (50 mg/kg, twice daily, 12 hr apart) at different schedules relative to the day of infection (day 0); i.e., from −3 to +7 (n = 9), −1 to +7 (n = 13), +1 to +10 (n = 6), and +3 to +7 (n = 7). Control mice received vehicle (PBS; n = 28). Six independent experiments with similar trend were performed.

(B) H&E staining of DPTA-treated (NO) and vehicle-treated control mice at the time of ECM onset in controls (630×).

(C) Mean microgram (μg) of Evans blue per gram (g) of tissue ± SD in mice receiving vehicle (Veh.; n = 12) or DPTA-NO (−1→7; n = 10; 3→7; n = 5) 7 days after PbA$^{EEF1\alpha\text{-}GFP}$ infection. Two independent experiments with similar trend were performed.

(D) Mean percentage of infected GFP$^+$ RBCs ± SD in the same mice as in (A).

(E) Mean relative number of *Plasmodium* 18S/*Gusb* mRNA in the brain of PbA$^{EEF1\alpha\text{-}GFP}$-infected mice receiving vehicle (n = 7) or DPTA-NO (−1→7; n = 7) ± SD. Two independent experiments with similar trend were performed.

(F) Luciferase activity in noninfected (NI) versus PbA$^{AMA1\text{-}GFP/LUC}$-infected mice (day 7) receiving vehicle (Veh.) or DPTA-NO (NO; −1→7). RLU, relative light units.

(G) Mean luciferase activity ± SD in the same mice as (F), with seven to nine mice per group. Two independent experiments with similar trend were performed.

(H) Mean luciferase activity ± SD in brains collected from the same mice as (F).

(I) Mean fold induction (relative to noninfected controls) ± SD of *Cd3e*, *Cd4*, and *Cd8α* mRNA normalized to *Gusb* mRNA, as assessed by quantitative real-time RT-PCR in the brain of noninfected mice (n = 7) or PbA$^{EEF1\alpha\text{-}GFP}$-infected mice receiving vehicle (PBS; n = 7) versus DPTA-NO (n = 7). Two independent experiments analyzed at day 7 after infection were performed.

*p < 0.05; **p < 0.01; ***p < 0.001. n.s., p > 0.05. See also Figure S1.

production; i.e., CO-Hb (Figure 2C). When used at a protective dosage/schedule, DPTA-NO failed to protect PbA$^{EEF1\alpha\text{-}GFP}$-infected HO-1-deficient (*Hmox1*$^{-/-}$) mice from succumbing to ECM (Figures 2D and 2E). Parasitemias were indistinguishable between *Hmox1*$^{+/+}$ *versus* *Hmox1*$^{-/-}$ mice receiving DPTA-NO or not (Figure 2F). This suggests that NO confers disease tolerance to *Plasmodium* infection via a mechanism that involves the induction of HO-1 expression.

NO Inhibits Neuroinflammation via a Mechanism Involving HO-1

NO inhibited the accumulation of activated T_H and T_C cells in the brain of PbA$^{EEF1\alpha\text{-}GFP}$-infected mice, as assessed by quantitative real-time RT-PCR for the expression of several effector molecules involved in the pathogenesis of ECM; i.e., *Ctla-4* (Jacobs et al., 2002), *Prf* (Nitcheu et al., 2003), and *GzmB* (Haque et al., 2011) (Figure 3A). A similar inhibitory effect was observed for other molecules involved in T_H and/or T_C activation and presumably therefore driving ECM, including *Icos*, *Cd28*, and Fas ligand (*Fasl*) (Figure 3A), among others (Figure S2). This immunomodulatory effect was lost in *Hmox1*$^{-/-}$ mice (Figures 3A and S2).

NO inhibited the expression of mRNA-encoding *Cd45* in the brain of infected *Hmox1*$^{+/+}$ mice, but not in *Hmox1*$^{-/-}$ mice, confirming that NO prevents overall leukocyte accumulation in the brain (Figure 3B). A similar inhibitory effect was observed for mRNAs encoding the chemokines *Mig/Cxcl9*, *Cxcl10/Ip-10*, and *Ccl2/Mcp1*, the chemokine receptor *Ccr7*, the proinflammatory cytokines *Tnf* and *Il-6*, as well as the costimulatory molecules *Cd80* and *Cd86*, in PbA$^{EEF1\alpha\text{-}GFP}$-infected *Hmox1*$^{+/+}$ mice, but not in *Hmox1*$^{-/-}$ mice (Figure 3B). NO also inhibited the expression of other genes involved in the

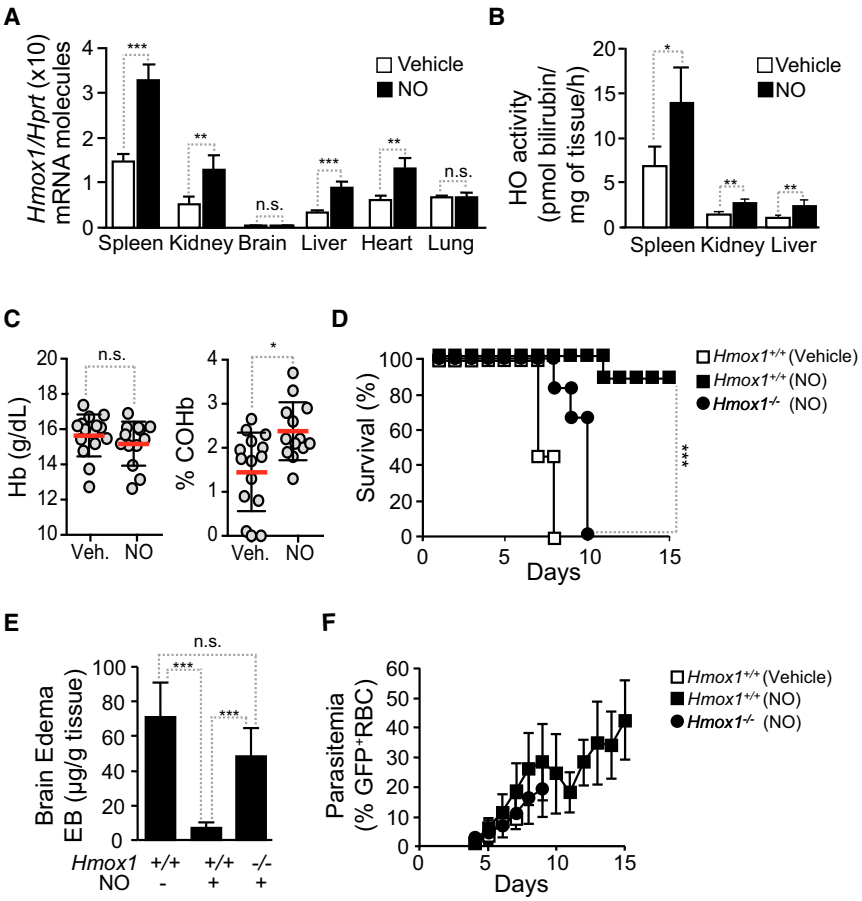

Figure 2. The Protective Effect of NO against ECM Is Mediated via HO-1 Expression

(A) Mean relative number of *Hmox1/Hprt* mRNA molecules ± SD in C57BL/6 mice receiving vehicle or DPTA-NO (50 mg/kg; twice 12 hr apart; n = 5 per group), as assessed by real-time qRT-PCR. Samples were collected 4 hr after the last DPTA-NO administration.

(B) Mean HO activity ± SD in mice treated as in (A) (n = 4 per group).

(C) Mean Hb concentration and percentage of CO-Hb ± SD in whole blood of C57BL/6 mice (n = 10) treated as in (A).

(D) Survival of PbA$^{EEF1\alpha\text{-}GFP}$-infected WT (*Hmox1*$^{+/+}$; n = 10) or HO-1-deficient (*Hmox1*$^{-/-}$; n = 6) C57BL/6 mice receiving DPTA-NO. Control *Hmox1*$^{+/+}$ mice received vehicle (PBS; n = 9). Two independent experiments were performed.

(E) Brain edema 7 days after PbA$^{EEF1\alpha\text{-}GFP}$ infection in Hmox1$^{+/+}$ (n = 5) versus Hmox1$^{-/-}$ (n = 4) mice receiving DPTA-NO (+; −1 to +7) or *Hmox1*$^{+/+}$ mice receiving vehicle (−; n = 7) as in (D). Edema is expressed as mean micrograms (µg) of Evans blue per gram (g) of tissue ± SD in one experiment.

(F) Mean percentage of infected GFP^{+} RBCs ± SD in the same mice as in (D).

*p < 0.05; **p < 0.01; ***p < 0.001. n.s., p > 0.05.

pathogenesis of ECM (Figure S2). This suggests that NO inhibits neuroinflammation associated with *Plasmodium* infection via a mechanism involving HO-1.

NO and CO Restrain T_H and T_C Cell Activation in Response to *Plasmodium* Infection

NO reduced the number of activated CD4^{+}CD44^{high}CD62L^{low} T_H cells expressing interferon γ (IFNγ) and CXCR3 in the spleen of PbA$^{EEF1\alpha\text{-}GFP}$-infected mice, as compared to infected vehicle-treated controls (Figure 4A). A similar effect was observed for activated CD8^{+}CD44^{high}CD62L^{low} T_C cells expressing GzmB and/or IFNγ (Figure 4B). NO did not reduce the total number of splenic lymphocytes in PbA$^{EEF1\alpha\text{-}GFP}$-infected mice, including T_H and T_C cells, dendritic cells, monocyte/macrophages, or polymorphonuclear cells, as compared to vehicle-treated controls (Figure S3A).

CO administration via inhalation mimicked to a large extent the immunoregulatory effect of NO, reducing the number of activated CD4^{+}CD44^{high}CD62L^{low} and CD4^{+}IFNγ T_H cells in the spleen of PbA$^{EEF1\alpha\text{-}GFP}$-infected mice, as compared to air-treated controls (Figure 4C). CO did not inhibit the expression of CXCR3 in activated T_H cells (Figure 4C). CO also reduced the number of activated CD8^{+}CD44^{high}CD62L^{low}, CD8^{+}GzmB^{+}, and CD8^{+}IFNγ^{+} T_C cells in the spleen of PbA$^{EEF1\alpha\text{-}GFP}$-infected mice, as compared to air-treated controls (Figure 4D). CO reduced the total number of lymphocytes and T_C cells in the spleen of infected mice, as compared to infected air-treated controls (Figure S3B). Given that (1) NO induces HO-1 (Figures 2A and 2B) and CO production (Figure 2C) and (2) CO mimics the immunoregulatory effect of NO during *Plasmodium* infection, we infer that this effect of NO is probably mediated via a mechanism involving CO. These data, however, do not prove that CO is necessary to support the immunoregulatory effect of NO.

The Protective Effect of NO Acts via a Mechanism Involving Nrf2

NO induces HO-1 expression in vitro (Motterlini et al., 1996) via a mechanism involving the transcription factor Nrf2 (Naughton et al., 2002). We asked whether a similar mechanism occurs in vivo to prevent the pathogenesis of ECM. *Nrf2* deletion in C57BL/6 mice impaired the induction of *Hmox1* mRNA in response to DPTA-NO, as assessed in different organs by quantitative real-time RT-PCR (Figure 5A). This correlated with lack of HO activity (Figure 5B), demonstrating that NO induces HO-1 and raises HO activity in vivo, via an Nrf2-dependent mechanism.

When administered at a protective dosage/schedule, NO failed to protect *Nrf2*$^{-/-}$ mice from succumbing to ECM (Figure 5C). Parasitemias were similar in *Nrf2*$^{-/-}$ *versus* *Nrf2*$^{+/+}$ mice receiving DPTA-NO or not (Figure 5D). Mortality of infected *Nrf2*$^{-/-}$ mice receiving DPTA-NO was associated with brain edema (Figure 5E). This suggests that Nrf2 activation by NO suppresses ECM and confers disease tolerance to *Plasmodium* infection.

CO administration restored the protective effect of DPTA-NO in PbA$^{EEF1\alpha\text{-}GFP}$-infected *Nrf2*$^{-/-}$ mice (Figure 5F), without

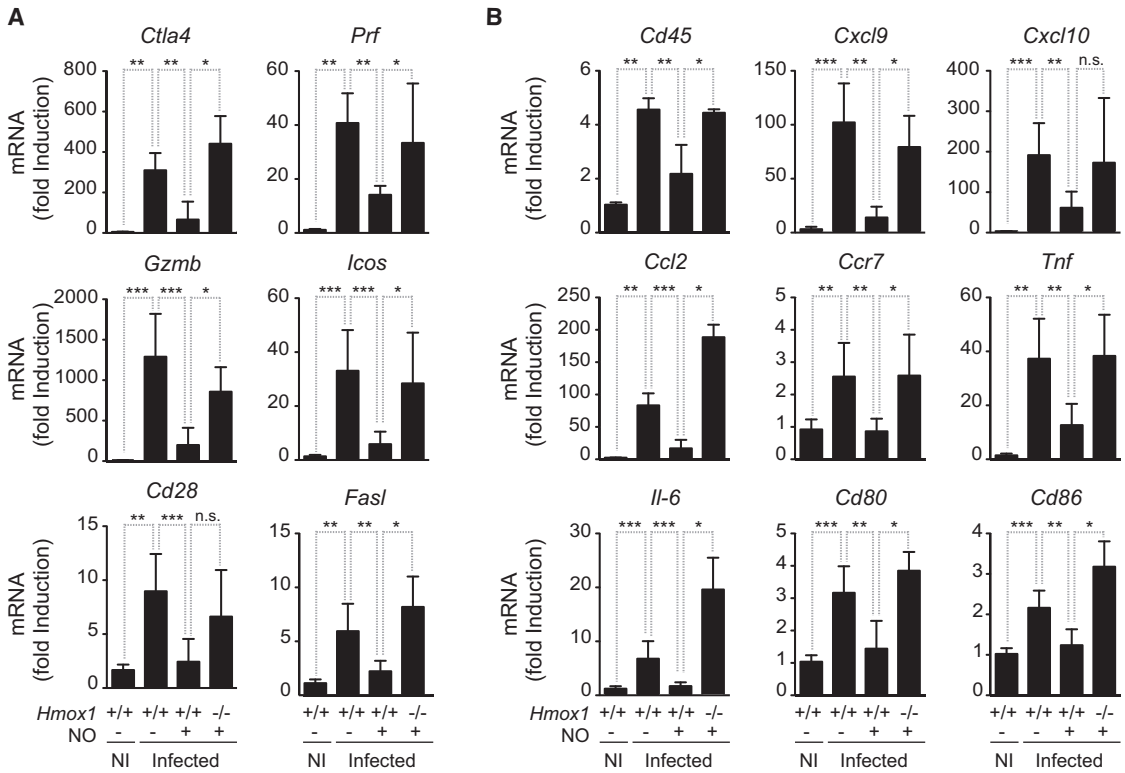

Figure 3. NO Inhibits Neuroinflammation via a Mechanism Involving HO-1

(A) T cell activation. Mean fold induction of mRNA expression (relative to noninfected mice) ± SD assessed by real-time qRT-PCR in the brains of noninfected *Hmox1*$^{+/+}$ mice (n = 7), PbA$^{EEF1\alpha\text{-}GFP}$-infected *Hmox1*$^{+/+}$ mice receiving vehicle (–; PBS; n = 7) or DPTA-NO (+; 50 mg/kg, twice daily, 12 hr apart; from days −1 to +7; n = 7) versus *Hmox1*$^{-/-}$ mice receiving DPTA-NO (+; n = 3). Expression values for each gene were normalized to Gusb mRNA. Two independent experiments with similar trend were performed.

(B) Neuroinflammation, determined as in (A). *p < 0.05; **p < 0.01; ***p < 0.001. n.s., p > 0.05. Notice that n = 3 for *Hmox1*$^{-/-}$ mice.

See also Figure S2.

interfering with parasitemia (Figure 5G). This suggests that the protective effect of NO against ECM is mediated via a mechanism that involves CO. These data, however, do not prove that CO is necessary to support the protective effect of Nrf2.

HO-1 Does Not Regulate NO Bioavailability during *Plasmodium* Infection

DPTA-NO administration increased the concentration of the two major end products of NO oxidation (i.e., nitrite and nitrate, in the plasma of noninfected or PbA$^{EEF1\alpha\text{-}GFP}$-infected mice) in comparison to vehicle-treated controls (Figure 6A). DPTA-NO administration was also associated with the accumulation, in the brain of PbA$^{EEF1\alpha\text{-}GFP}$-infected mice, of the end product of the NO-regulated enzyme guanylate cyclase cyclic guanosine monophosphate (cGMP) (Figure 6B) (Gramaglia et al., 2006). Concentration of nitrite/nitrate in the plasma of PbA$^{EEF1\alpha\text{-}GFP}$-infected *Hmox1*$^{-/-}$ or *Nrf2*$^{-/-}$ mice was similar to that of wild-type (WT) controls (Figure 6A). The same was true for cGMP accumulation in the brain (Figure 6B). This suggests that expression of Nrf2-regulated genes, including HO-1, does not modulate NO bioavailability during *Plasmodium* infection. Moreover, this excludes that failure of NO to suppress the pathogenesis of ECM in *Hmox1*$^{-/-}$ or *Nrf2*$^{-/-}$ mice is due to a putative reduction of NO availability.

Nrf2 and HO-1 Limit the Pro-oxidant Effect of NO Exerted on Cell-free Hb

Although NO and CO target cell-free Hb, they should act in opposite ways, with NO propagating Hb oxidation and CO preventing it (Hebbel et al., 1988; Pamplona et al., 2007). NO increased the concentration of MetHb in the plasma of noninfected as well as in PbA$^{EEF1\alpha\text{-}GFP}$-infected WT mice, as compared to vehicle-treated controls (Figure 6C). This effect was exacerbated in infected *Hmox1*$^{-/-}$ or *Nrf2*$^{-/-}$ mice versus WT controls (Figure 6C). This suggests that regulation of HO-1 expression by Nrf2 restrains the oxidation of cell-free Hb by NO, during *Plasmodium* infection.

PbA$^{EEF1\alpha\text{-}GFP}$ infection was associated with the accumulation of non-Hb-bound heme (i.e., free heme), in the plasma of WT mice (Figure 6D). This effect was exacerbated in *Hmox1*$^{-/-}$ and in *Nrf2*$^{-/-}$ mice versus WT controls, receiving NO or not (Figure 6D). This suggests that regulation of HO-1 expression by Nrf2 restrains NO from oxidizing Hb (Figure 6C), presumably inhibiting the release of its prosthetic heme groups during

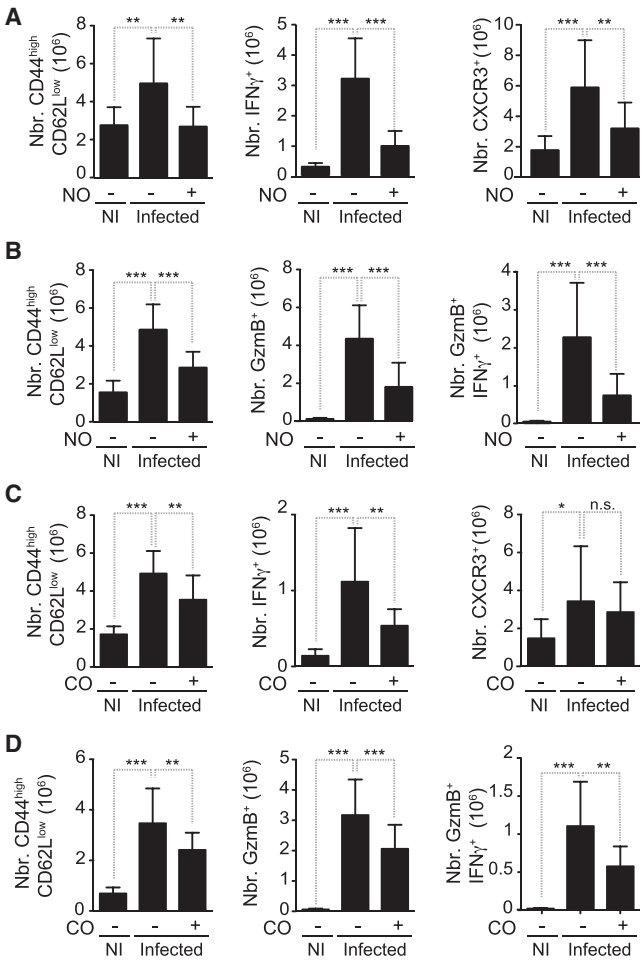

Figure 4. NO and CO Restrain T_H and T_C Cell Activation in Response to *Plasmodium* Infection

(A–D) Mean number of splenic (A) TCRβ$^+$CD4$^+$ T_H cells or (B) TCRβ$^+$CD8$^+$ T_C cells expressing different activation markers ± SD in noninfected mice (n = 12) or PbA$^{EEF1\alpha\text{-}GFP}$-infected mice receiving vehicle (n = 17) versus DPTA-NO (+; 50 mg/kg, twice daily, 12 hr apart, from days −1 to 5; n = 15). Mean number of splenic (C) TCRβ$^+$CD4$^+$ T_H cells or (D) TCRβ$^+$CD8$^+$ T_C cells expressing different activation markers ± SD in noninfected mice (n = 13) or PbA$^{EEF1\alpha\text{-}GFP}$-infected mice exposed to air (n = 15) versus CO (250 ppm, from days 3 to 5.5 post-infection; n = 15). Analyses were performed by flow cytometry 5.5 days after infection in three independent experiments with similar trend. *p < 0.05; **p < 0.01; ***p < 0.001. n.s., p > 0.05.

See also Figure S3.

Plasmodium infection, an effect that should contribute to the protective effect of NO against ECM (Ferreira et al., 2008).

The Protective Effect of CO against ECM Acts Independently of NO

We assessed whether the protective effect of CO against ECM acts via a mechanism involving endogenous NO production by different NOS. CO administration via inhalation protected PbA$^{EEF1\alpha\text{-}GFP}$-infected mice carrying combined deletions of *Nos* alleles (i.e., *Nos1/Nos2*$^{-/-}$ (Figure 7A), *Nos2/Nos3*$^{-/-}$ (Figure 7B), and *Nos1/Nos3*$^{-/-}$ [Figure 7C]) from succumbing to ECM. Similar effects were observed in *Nos1*$^{-/-}$ (Figure S4A), *Nos2*$^{-/-}$ (Figure S4B), and *Nos3*$^{-/-}$ (Figure S4C) mice. The protective effect of CO was associated with inhibition of brain edema (Figures 7D and S4D), suggesting that CO is sufficient and likely acts downstream of NO to suppress the pathogenesis of ECM. This observation also suggests that the protective effect of CO does not require endogenous NO production, although this has not been established conclusively.

Time of ECM onset was delayed in mice carrying a deletion of the neuronal *Nos1* allele (i.e., *Nos1*$^{-/-}$ (Figure S4A), *Nos1/Nos2*$^{-/-}$ [Figure 7A], and *Nos1/Nos3*$^{-/-}$ [Figure 7C] mice) in comparison to genotype-matched controls carrying a functional *Nos1* allele (Figures S4A, 7A, and 7C). Neither *Nos2* (*Nos2*$^{-/-}$) nor *Nos3* (*Nos3*$^{-/-}$) deletions influenced ECM onset or parasitemias in comparison to genotype-matched WT controls (Figures S4B, S4C, and 7B).

DISCUSSION

When used pharmacologically, NO (Cabrales et al., 2011; Gramaglia et al., 2006; Ong et al., 2013) and CO (Ferreira et al., 2008, 2011; Pamplona et al., 2007) suppress the pathogenesis of ECM. The mechanism(s) underlying this salutary effect and the potential use of these gasotransmitters as adjunctive therapies to treat severe forms of malaria in humans remain to be established (Hawkes et al., 2011).

The term gasotransmitter as used hereby refers to biologic active gaseous molecules produced physiologically (Mustafa et al., 2009). NO is generated by the enzymatic conversion of L-arginine and molecular oxygen to L-citrulline, catalyzed by different NOS isoforms, whereas CO is generated through the enzymatic conversion of heme and molecular oxygen, catalyzed by different HO isoforms (Tenhunen et al., 1968). In contrast to CO, NO is a labile-free radical with potentially deleterious pro-oxidant activity (Figure 6C) (Gladwin et al., 2004) that can act locally in the brain to promote the pathogenesis of CM. Consistent with this notion, stable end products of NO accumulate in the cerebral spinal fluid of individuals with adverse disease outcome from CM (Weiss et al., 1998). Moreover, deletion of the neuronal NOS isoform (i.e., *Nos1*, confers some level of protection against ECM [Figures 7 and S4]), suggesting that when produced locally in the brain, NO is deleterious and promotes, rather than protects from, ECM.

When applied pharmacologically to mice, NO acts systemically to suppress the pathogenesis of ECM (Figure 1) (Cabrales et al., 2011; Gramaglia et al., 2006; Ong et al., 2013). This suggests that whereas NO can act systemically to confer protection against malaria, its bioavailability during *Plasmodium* infection is not sufficient to afford this salutary effect. This is attributed most likely to NO scavenging by cell-free Hb (Patel and Gladwin, 2004; Gramaglia et al., 2006) as well as to reduction of NOS2 expression (Weiss et al., 1994), presumably driven by cellular iron overload (Gozzelino et al., 2012; Gozzelino and Soares, 2014). Reduced NO bioavailability promotes brain microvascular constriction, thus fostering the pathogenesis of ECM (Cabrales et al., 2011; Gramaglia et al., 2006; Ong et al., 2013). NO administration compensates for reduced systemic NO bioavailability during *Plasmodium* infection, preventing the pathogenesis of ECM.

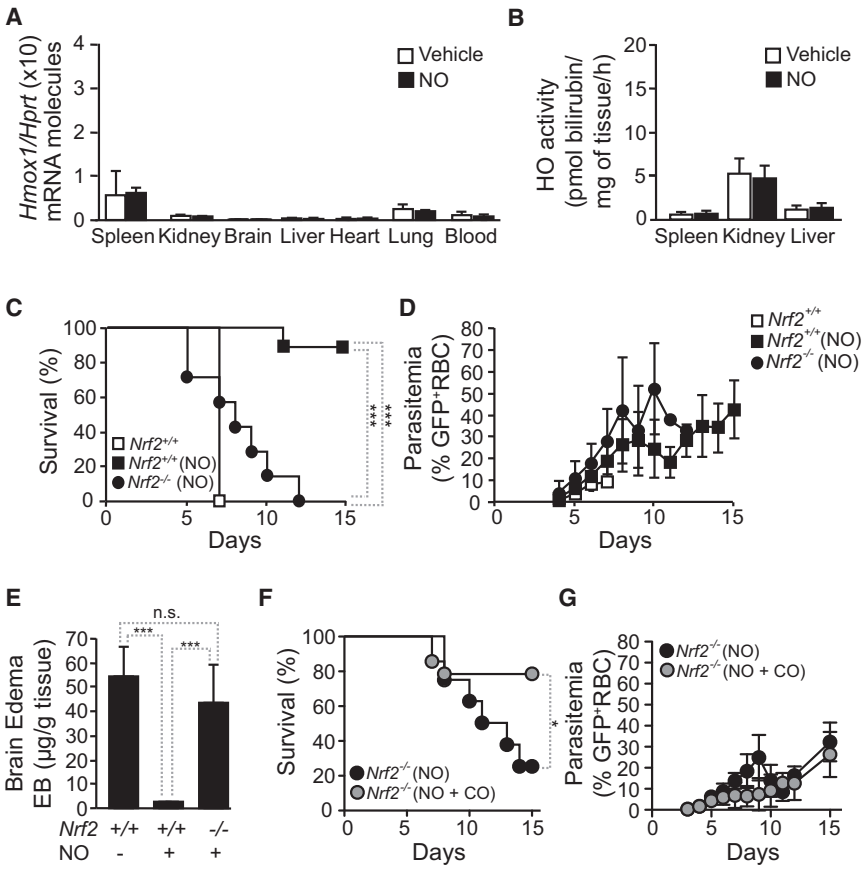

Figure 5. The Protective Effect of NO Is Mediated via HO-1 Induction by Nrf2

(A) Mean number of *Hmox1*/*Hprt* mRNA molecules ± SD in Nrf2-deficient ($Nrf2^{-/-}$) mice receiving vehicle or DPTA-NO (NO; 50 mg/kg twice 12 hr apart; n = 5 per group), as assessed by qRT-PCR. Samples were collected 4 hr after the last DPTA-NO administration. The y axis scale is the same as in Figure 2A, for comparison.

(B) HO activity is shown as mean pmol bilirubin/mg of tissue/hr ± SD in mice treated as in (A) (n = 4 mice per group). The y axis scale is the same as in Figure 2B, for comparison.

(C) Survival of $PbA^{EEF1\alpha\text{-}GFP}$-infected $Nrf2^{+/+}$ mice (n = 9) versus $Nrf2^{-/-}$ mice (n = 7) receiving DPTA-NO (NO: 50 mg/kg, twice daily, 12 hr apart, days −1 to +7) or $Nrf2^{+/+}$ mice receiving vehicle (PBS; n = 8). Two independent experiments with similar trend were performed.

(D) Mean percentage of infected RBCs ± SD in the same mice as in (C).

(E) Brain edema 7 days in $PbA^{EEF1\alpha\text{-}GFP}$-infected $Nrf2^{+/+}$ mice receiving vehicle (PBS; n = 3) or DPTA-NO (NO; +; −1 to +7) versus $Nrf2^{-/-}$ mice receiving DPTA-NO (+; NO; −1 to +7; n = 3). Edema is expressed as mean micrograms (µg) of Evans blue per gram (g) of tissue ± SD; data are derived from one experiment.

(F) Survival of $PbA^{EEF1\alpha\text{-}GFP}$-infected $Nrf2^{-/-}$ mice receiving DPTA-NO (NO) and exposed to air (n = 8) or CO (250 ppm, from days 3 to 6 postinfection; n = 14). Two independent experiments with similar trend were performed.

(G) Mean percentage of infected RBCs ± SD in the same mice as in (F).

*p < 0.05; ***p < 0.001. n.s., p > 0.05.

Although we confirmed that NO administration suppresses the pathogenesis of ECM (Figure 1) (Cabrales et al., 2011; Gramaglia et al., 2006; Ong et al., 2013), we found that this protective effect relies on the induction of HO-1 (Figure 2), via a mechanism involving the transcription factor Nrf2 (Figure 5). Induction of HO-1 leads to the production of CO (Figure 2) (Motterlini et al., 1996), a gasotransmitter that suppresses the pathogenesis of ECM (Figures 5, 7, and S4). NO acts most likely as a "double-edged" sword during *Plasmodium* infection, promoting Hb oxidation (Figure 6C) as well as the expression of HO-1 and the production of CO (Figure 2), limiting Hb oxidation (Figure 6D). Presumably, HO-1 and CO contribute to the protective effect of NO (Figures 2 and 5) by suppressing Hb oxidation and heme release from Hb, thus preventing heme from partaking in the pathogenesis of ECM (Ferreira et al., 2008, 2011; Pamplona et al., 2007). These effects of HO-1 and CO, which limit the pro-oxidant effect of NO, probably allow this gasotransmitter to exert additional salutary effects that act irrespectively of HO-1 and CO.

NO has no apparent impact on pathogen load, suggesting that this gasotransmitter confers disease tolerance to the blood stage of *Plasmodium* infection (Figure 1). However, NO reduces parasite sequestration in the brain (Figures 1H and S1D), a salutary effect that should contribute to suppressing the onset of ECM as well as that of CM (Miller et al., 2013). NO also inhibits the activation, proliferation, and expansion of pathogenic T_H and T_C in the spleen during the blood stage of *Plasmodium* infection (Figure 4). This prevents the accumulation of T_H and T_C cells in the brain of infected mice (Figure 1), reducing neuroinflammation (Figure 3) and, as such, suppressing the pathogenesis of ECM (Miller et al., 2013). This salutary effect is probably exerted via the pro-oxidant activity of NO, which suppresses T cell responses (Hoffman et al., 1990) through the induction of T cell apoptosis (Brito et al., 1999). NO may also act indirectly, via the induction of HO-1, to induce T cell apoptosis (McDaid et al., 2005; Soares et al., 2009).

When applied to *Nos1*-deficient mice (i.e., $Nos1^{-/-}$, *Nos1*/$Nos2^{-/-}$, or *Nos1*/$Nos3^{-/-}$), CO exerts a negative impact on parasitemia (Figures S4A, 7A, and 7C). This effect is only observed in Nos1-deficient mice, presumably because a small fraction of these mice escapes ECM (Figures S4A, 7A, and 7C), thus allowing for comparison of parasitemia over time. This suggests that CO modulates not only disease tolerance, early during *Plasmodium* infection (i.e., preventing CM without impacting on pathogen load) but also resistance (i.e., reducing pathogen load) later on, in comparison to control mice that do receive CO. This latter effect of CO may be exerted via a direct interaction of this gasotransmitter with the pathogen or indirectly via modulation of host-resistance mechanisms (Soares et al., 2009).

In conclusion, the salutary effect exerted by NO during *Plasmodium* infection is mediated to at least some extent, indirectly,

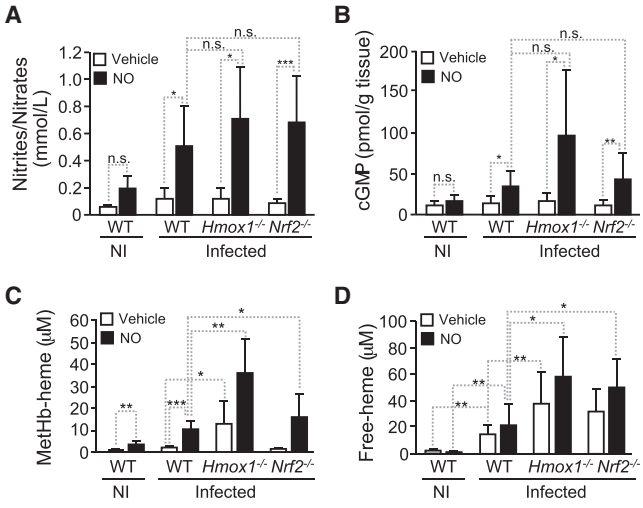

Figure 6. HO-1 and Nrf2 Do Not Modulate NO Bioavailability during *Plasmodium* Infection while Restraining Hb Oxidation and Heme Release

(A) Mean ratio of nitrite-to-nitrate concentration ± SD in the plasma of noninfected (NI) WT C57BL/6 mice receiving vehicle (PBS; n = 10) or DPTA-NO (NO; 50 mg/kg twice daily, 12 hr apart from day −1 to +6: n = 10) versus $PbA^{EEF1\alpha\text{-}GFP}$-infected WT, HO-1-deficient ($Hmox1^{-/-}$), or Nrf2-deficient ($Nrf2^{-/-}$) C57BL/6 mice receiving DPTA-NO (n = 12 for WT, n = 8 for $Hmox1^{-/-}$ and n = 14 for $Nrf2^{-/-}$) or vehicle (n = 14 for WT, n = 9 for $Hmox1^{-/-}$ and n = 12 for $Nrf2^{-/-}$). Three independent experiments with similar trend were performed.

(B) Mean cGMP ± SD in noninfected (NI) WT C57BL/6 mice receiving vehicle (n = 10) or DPTA-NO (NO, n = 10) versus $PbA^{EEF1\alpha\text{-}GFP}$-infected WT, $Hmox1^{-/-}$, or $Nrf2^{-/-}$ mice receiving DPTA-NO (n = 13 for WT, n = 7 for $Hmox1^{-/-}$ mice and n = 12 for $Nrf2^{-/-}$ mice) or vehicle (n = 14 for WT, n = 9 for $Hmox1^{-/-}$ mice and n = 12 for $Nrf2^{-/-}$ mice). Three independent experiments were performed. NO donor DPTA-NO was administered from day −1 to day 6 postinfection.

(C) Mean concentration of MetHb ± SD in the plasma of noninfected or $PbA^{EEF1\alpha\text{-}GFP}$-infected mice receiving vehicle (PBS) or DPTA-NO (NO; 50 mg/kg twice daily, 12 hr apart from day −1 to +6). Measurements were taken on day 6 postinfection. Three experiments (n = 5–12 mice per group) with similar trend were performed.

(D) Mean concentration of non-Hb-bound (free) heme ± SD in the plasma of the same mice as in (C).

*p < 0.05; **p < 0.01; ***p < 0.001. n.s., p > 0.05.

by CO. This interplay between the two gasotransmitters should be taken into consideration when envisioning their therapeutic application as adjunctive therapies against severe forms of malaria.

EXPERIMENTAL PROCEDURES

Mice

Mice were bred and maintained under specific pathogen-free (SPF) conditions. Protocols were approved by the Ethics Committee of the Instituto Gulbenkian de Ciência (A008.2010 and A009.2011) and by the Portuguese National Entity (Direção Geral de Alimentação e Veterinária; 008959 and 018071). All experiments were performed according to the Portuguese (Decreto-Lei 113/2013) and European (Directive 2010/63/EU) legislations.

Parasites, Infection, and Disease Assessment

Mice were infected by intraperitoneal (i.p.) inoculation of 10^5 RBCs infected with transgenic PbA strains $PbA^{EEF1\alpha\text{-}GFP}$ (259cl1; MR4; MRA-865) (Franke-Fayard et al., 2004) or $PbA^{AMA1\text{-}GFP/LUC}$ (1037cl1) (Spaccapelo et al., 2010). Parasitemias were determined by flow cytometry (Ferreira et al., 2011) and/or by Giemsa-stained blood smears. Mice were monitored daily for clinical signs of ECM, including hemi- or paraplegia, head deviation, tendency to rollover on stimulation, ataxia, and convulsions. The day of infection is zero (0) in all experiments.

NO Treatment

Mice received DPTA-NO (Alexis Biochemicals) i.p. (50 mg/kg of body weight dissolved in 200 μl of PBS) twice daily with different schedules as indicated in the figures. DPTA-NO was prepared freshly in ice-cold PBS and injected immediately thereafter.

CO Treatment

Mice were placed in a gastight 60-liter capacity chamber and exposed continuously between days 3 and 6 postinfection to CO at a flow rate of ~12 l/min (final concentration of 250 ppm) (Sato et al., 2001). CO concentration was monitored continuously using a CO analyzer (Interscan).

Luciferase Imaging

Mice were infected with $PbA^{AMA1\text{-}GFP/LUC}$, treated with vehicle or DPTA-NO (day −1 to +7), and luciferase activity was determined at the time of ECM onset in control mice (i.e., day 7). Luciferase activity was visualized by whole-mice imaging or in dissected tissues using an electron-multiplying charge-coupled device (EM-CCD) photon-counting camera (ImagEM; Hamamatsu).

Brain Edema

Brain edema was evaluated using Evans blue, administered intravenously (2% solution, 100 μl; Sigma-Aldrich), as described by Pamplona et al. (2007).

HO-1 Activity

Mice were injected (i.p.) with DPTA-NO or vehicle twice 12 hr apart, and HO activity was measured 4 hr thereafter in tissues snap-frozen in liquid nitrogen, as described by Sato et al. (2001).

Endogenous CO Production

Mice were treated with vehicle or DPTA-NO as detailed for HO-1 activity determination. Blood was collected from the facial vein (200 μl) into a heparinized tube (10 μl), transferred to an assay cuvette, and analyzed using an Avoximeter 4000 (ITC) for total Hb (g/dl) and CO-Hb (percentage of total Hb) content.

Histology

Brains were harvested when clinical signs of ECM were observed in control mice. Tissue was fixed in buffered 4% (v/v) paraformaldehyde and embedded in paraffin. Paraffin sections were cut at 12 μm, stained with hematoxylin and eosin (H&E), and analyzed via an Olympus BX51 light microscope.

Quantitative Real-Time PCR

Mice were sacrificed at the day of ECM onset in control mice. Total RNA was isolated from the different organs using TRIzol (Invitrogen Life Technologies) and the RNeasy Mini Kit (QIAGEN) and used to synthesize cDNA for PCR with Power SYBR Green PCR master mix (Invitrogen Life Technologies). Transcript number was calculated from the threshold cycle (Ct) of each gene with a $2^{-\Delta\Delta CT}$ method (relative number) and normalized to hypoxanthine-guanine phosphoribosyltransferase (*Hprt*) or glucuronidase β (*Gusb*).

Mouse Immune Quantitative RT-PCR Array

TaqMan gene signature mouse immune array (Applied Biosystems) was used to quantify all other mRNAs according to manufacturer's recommendations (Ferreira et al., 2011). Gene expression was determined as above.

T Cell Activation

Analyses of T cell activation were performed in the spleens of naive or $PbA^{EEF1\alpha\text{-}GFP}$-infected C57BL/6 mice at 5.5 days postinfection, as described in Ferreira et al. (2011).

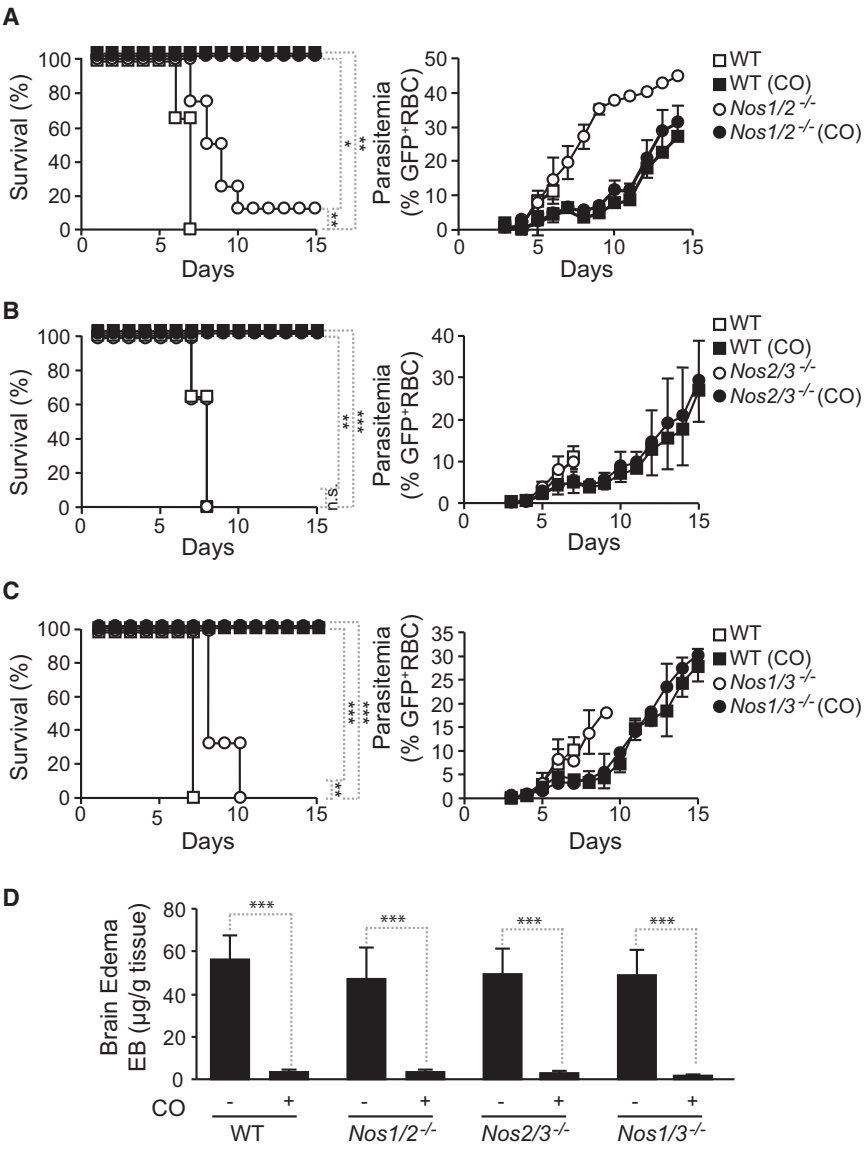

Figure 7. CO Confers Protection against ECM in Double NOS-Deficient Mice

(A) Survival and mean parasitemia ± SD of PbA$^{EEF1\alpha\text{-}GFP}$-infected WT (*Nos1/Nos2*$^{+/+}$) versus Nos1/Nos2$^{-/-}$ mice exposed to air (n = 9 for WT; n = 8 for *Nos1/Nos2*$^{-/-}$) or CO (250 ppm, from day 3 to 6 postinfection; n = 4 for WT; n = 4 for *Nos1/Nos2*$^{-/-}$). Two independent experiments with similar trend were performed.

(B) Survival and mean parasitemia ± SD of PbA$^{EEF1\alpha\text{-}GFP}$-infected WT (*Nos2/Nos3*$^{+/+}$) versus Nos2/Nos3$^{-/-}$ mice exposed to air (n = 14 for WT; n = 8 for *Nos2/Nos3*$^{-/-}$) or CO (n = 4 for WT; n = 8 for *Nos2/Nos3*$^{-/-}$). Three independent experiments with similar trend were performed.

(C) Survival and mean parasitemia ± SD of PbA$^{EEF1\alpha\text{-}GFP}$-infected WT (*Nos1/Nos3*$^{+/+}$) versus Nos1/Nos3$^{-/-}$ mice exposed to air (n = 9 for WT; n = 5 for *Nos1/Nos3*$^{-/-}$) or CO (n = 4 for WT; n = 2 for *Nos1/Nos3*$^{-/-}$). Two independent experiments were performed.

(D) Brain edema quantified by Evans blue accumulation in the brain parenchyma of PbA$^{EEF1\alpha\text{-}GFP}$-infected WT, Nos1/Nos2$^{-/-}$, Nos2/Nos3$^{-/-}$, and Nos1/Nos3$^{-/-}$ mice receiving air (–) or CO (+). Panel shows mean micrograms (µg) of Evans blue per gram (g) of brain tissue ± SD. Two independent experiments with similar trend were performed. When indicated, mice received CO via inhalation between day 3 and day 6 postinfection (250 ppm, 24 hr/day). n = 5 mice per group.

*p < 0.05; **p < 0.01; ***p < 0.001. n.s., p > 0.05. See also Figure S4.

Statistics

Survival curves were represented as Kaplan-Meier plots, and significance was evaluated with the log rank (Mantel-Cox) test. Comparison of the means of three or more groups was performed using one-way ANOVA, and significance between every two groups was assessed by the Bonferroni multiple comparison test when data assumed Gaussian distribution, as assessed by the D'Agostino and Pearson omnibus normality test. For samples with a "(n)" not allowing to ascertain Gaussian distribution, group comparison was analyzed using the Kruskal-Wallis test, followed by Mann-Whitney U test for assessment of significance between every two groups. Outliers were identified with the Grubbs' test from the GraphPad software, available online (http://graphpad.com/quickcalcs/Grubbs1.cfm). All tests were performed with the GraphPad v.5.0a software (Prism), and p values were represented as *p < 0.05, **p < 0.01, and ***p < 0.001.

SUPPLEMENTAL INFORMATION

Supplemental Information includes Supplemental Experimental Procedures and four figures and can be found with this article online at http://dx.doi.org/10.1016/j.celrep.2014.05.054.

AUTHOR CONTRIBUTIONS

V.J. and S. Ramos performed all the experimental work with help from M.-L.B., A.F., and V.O.-M. and contributed to the study design. S. Rebelo and S.C. generated and maintained all mouse colonies with V.J. J.T. and I.B. performed pathological analyses. C.J.J. provided the *Plasmodium* strains. M.P.S. formulated the original hypothesis, supervised the study design, and wrote the manuscript with V.J. and S. Ramos. All authors read and approved the manuscript.

ACKNOWLEDGMENTS

The authors thank Gabriel Martins (Cell Imaging Unit, Instituto Gulbenkian de Ciência) for technical support in the analyses of luciferase bioimaging and Sergio Duarte for slider image artwork. This work was supported by Fundação para a Ciência e Tecnologia grants PTDC/SAU-FCF/100762/2008, PTDC/SAU-TOX/116627/2010, HMSP-ICT/0018/2011, and RECI-IMI-IMU-0038-2012 to M.P.S.; SAU-MII/65765/2006 fellowship to V.O.-M.; Marie Curie 220152 GASMALARIA to V.J.; European Community Seventh Framework

grant ERC-2011-AdG. 294709-DAMAGECONTROL to M.P.S.; and European Social Fund TÁMOP-4.2.2.A-11/1/KONV-2012-0045 to V.J.

Received: March 26, 2014
Revised: April 23, 2014
Accepted: May 29, 2014
Published: June 26, 2014

REFERENCES

Andrade, B.B., Araújo-Santos, T., Luz, N.F., Khouri, R., Bozza, M.T., Camargo, L.M., Barral, A., Borges, V.M., and Barral-Netto, M. (2010). Heme impairs prostaglandin E2 and TGF-beta production by human mononuclear cells via Cu/Zn superoxide dismutase: insight into the pathogenesis of severe malaria. J. Immunol. *185*, 1196–1204.

Anstey, N.M., Weinberg, J.B., Hassanali, M.Y., Mwaikambo, E.D., Manyenga, D., Misukonis, M.A., Arnelle, D.R., Hollis, D., McDonald, M.I., and Granger, D.L. (1996). Nitric oxide in Tanzanian children with malaria: inverse relationship between malaria severity and nitric oxide production/nitric oxide synthase type 2 expression. J. Exp. Med. *184*, 557–567.

Ayres, J.S., and Schneider, D.S. (2012). Tolerance of infections. Annu. Rev. Immunol. *30*, 271–294.

Balla, J., Jacob, H.S., Balla, G., Nath, K., Eaton, J.W., and Vercellotti, G.M. (1993). Endothelial-cell heme uptake from heme proteins: induction of sensitization and desensitization to oxidant damage. Proc. Natl. Acad. Sci. USA *90*, 9285–9289.

Belcher, J.D., Chen, C., Nguyen, J., Milbauer, L., Abdulla, F., Alayash, A.I., Smith, A., Nath, K.A., Hebbel, R.P., and Vercellotti, G.M. (2014). Heme triggers TLR4 signaling leading to endothelial cell activation and vaso-occlusion in murine sickle cell disease. Blood *123*, 377–390.

Belnoue, E., Kayibanda, M., Vigario, A.M., Deschemin, J.C., van Rooijen, N., Viguier, M., Snounou, G., and Rénia, L. (2002). On the pathogenic role of brain-sequestered alphabeta CD8+ T cells in experimental cerebral malaria. J. Immunol. *169*, 6369–6375.

Belnoue, E., Potter, S.M., Rosa, D.S., Mauduit, M., Grüner, A.C., Kayibanda, M., Mitchell, A.J., Hunt, N.H., and Rénia, L. (2008). Control of pathogenic CD8+ T cell migration to the brain by IFN-gamma during experimental cerebral malaria. Parasite Immunol. *30*, 544–553.

Brito, C., Naviliat, M., Tiscornia, A.C., Vuillier, F., Gualco, G., Dighiero, G., Radi, R., and Cayota, A.M. (1999). Peroxynitrite inhibits T lymphocyte activation and proliferation by promoting impairment of tyrosine phosphorylation and peroxynitrite-driven apoptotic death. J. Immunol. *162*, 3356–3366.

Bunn, H.F., and Jandl, J.H. (1968). Exchange of heme among hemoglobins and between hemoglobin and albumin. J. Biol. Chem. *243*, 465–475.

Cabrales, P., Zanini, G.M., Meays, D., Frangos, J.A., and Carvalho, L.J. (2011). Nitric oxide protection against murine cerebral malaria is associated with improved cerebral microcirculatory physiology. J. Infect. Dis. *203*, 1454–1463.

Campanella, G.S., Tager, A.M., El Khoury, J.K., Thomas, S.Y., Abrazinski, T.A., Manice, L.A., Colvin, R.A., and Luster, A.D. (2008). Chemokine receptor CXCR3 and its ligands CXCL9 and CXCL10 are required for the development of murine cerebral malaria. Proc. Natl. Acad. Sci. USA *105*, 4814–4819.

Dhangadamajhi, G., Mohapatra, B.N., Kar, S.K., and Ranjit, M. (2009). Genetic variation in neuronal nitric oxide synthase (nNOS) gene and susceptibility to cerebral malaria in Indian adults. Infect. Genet. Evol. *9*, 908–911.

Dhangadamajhi, G., Mohapatra, B.N., Kar, S.K., and Ranjit, M.R. (2010). A new allele (eNOS4e) in the intron 4 (VNTR) of eNOS gene in malaria infected individuals of the population of Orissa (an eastern Indian state). Nitric Oxide *22*, 58–59.

Ferreira, A., Balla, J., Jeney, V., Balla, G., and Soares, M.P. (2008). A central role for free heme in the pathogenesis of severe malaria: the missing link? J. Mol. Med. *86*, 1097–1111.

Ferreira, A., Marguti, I., Bechmann, I., Jeney, V., Chora, A., Palha, N.R., Rebelo, S., Henri, A., Beuzard, Y., and Soares, M.P. (2011). Sickle hemoglobin confers tolerance to *Plasmodium* infection. Cell *145*, 398–409.

Figueiredo, R.T., Fernandez, P.L., Mourao-Sa, D.S., Porto, B.N., Dutra, F.F., Alves, L.S., Oliveira, M.F., Oliveira, P.L., Graça-Souza, A.V., and Bozza, M.T. (2007). Characterization of heme as activator of Toll-like receptor 4. J. Biol. Chem. *282*, 20221–20229.

Francis, S.E., Sullivan, D.J., Jr., and Goldberg, D.E. (1997). Hemoglobin metabolism in the malaria parasite *Plasmodium falciparum*. Annu. Rev. Microbiol. *51*, 97–123.

Franke-Fayard, B., Trueman, H., Ramesar, J., Mendoza, J., van der Keur, M., van der Linden, R., Sinden, R.E., Waters, A.P., and Janse, C.J. (2004). A *Plasmodium berghei* reference line that constitutively expresses GFP at a high level throughout the complete life cycle. Mol. Biochem. Parasitol. *137*, 23–33.

Gladwin, M.T., Crawford, J.H., and Patel, R.P. (2004). The biochemistry of nitric oxide, nitrite, and hemoglobin: role in blood flow regulation. Free Radic. Biol. Med. *36*, 707–717.

Gozzelino, R., and Soares, M.P. (2014). Coupling heme and iron metabolism via ferritin H chain. Antioxid. Redox Signal. *20*, 1754–1769.

Gozzelino, R., Jeney, V., and Soares, M.P. (2010). Mechanisms of cell protection by heme oxygenase-1. Annu. Rev. Pharmacol. Toxicol. *50*, 323–354.

Gozzelino, R., Andrade, B.B., Larsen, R., Luz, N.F., Vanoaica, L., Seixas, E., Coutinho, A., Cardoso, S., Rebelo, S., Poli, M., et al. (2012). Metabolic adaptation to tissue iron overload confers tolerance to malaria. Cell Host Microbe *12*, 693–704.

Gramaglia, I., Sobolewski, P., Meays, D., Contreras, R., Nolan, J.P., Frangos, J.A., Intaglietta, M., and van der Heyde, H.C. (2006). Low nitric oxide bioavailability contributes to the genesis of experimental cerebral malaria. Nat. Med. *12*, 1417–1422.

Haque, A., Best, S.E., Unosson, K., Amante, F.H., de Labastida, F., Anstey, N.M., Karupiah, G., Smyth, M.J., Heath, W.R., and Engwerda, C.R. (2011). Granzyme B expression by CD8+ T cells is required for the development of experimental cerebral malaria. J. Immunol. *186*, 6148–6156.

Hawkes, M., Opoka, R.O., Namasopo, S., Miller, C., Thorpe, K.E., Lavery, J.V., Conroy, A.L., Liles, W.C., John, C.C., and Kain, K.C. (2011). Inhaled nitric oxide for the adjunctive therapy of severe malaria: protocol for a randomized controlled trial. Trials *12*, 176.

Hebbel, R.P., Morgan, W.T., Eaton, J.W., and Hedlund, B.E. (1988). Accelerated autoxidation and heme loss due to instability of sickle hemoglobin. Proc. Natl. Acad. Sci. USA *85*, 237–241.

Hobbs, M.R., Udhayakumar, V., Levesque, M.C., Booth, J., Roberts, J.M., Tkachuk, A.N., Pole, A., Coon, H., Kariuki, S., Nahlen, B.L., et al. (2002). A new NOS2 promoter polymorphism associated with increased nitric oxide production and protection from severe malaria in Tanzanian and Kenyan children. Lancet *360*, 1468–1475.

Hoffman, R.A., Langrehr, J.M., Billiar, T.R., Curran, R.D., and Simmons, R.L. (1990). Alloantigen-induced activation of rat splenocytes is regulated by the oxidative metabolism of L-arginine. J. Immunol. *145*, 2220–2226.

Itoh, K., Chiba, T., Takahashi, S., Ishii, T., Igarashi, K., Katoh, Y., Oyake, T., Hayashi, N., Satoh, K., Hatayama, I., et al. (1997). An Nrf2/small Maf heterodimer mediates the induction of phase II detoxifying enzyme genes through antioxidant response elements. Biochem. Biophys. Res. Commun. *236*, 313–322.

Itoh, K., Wakabayashi, N., Katoh, Y., Ishii, T., Igarashi, K., Engel, J.D., and Yamamoto, M. (1999). Keap1 represses nuclear activation of antioxidant responsive elements by Nrf2 through binding to the amino-terminal Neh2 domain. Genes Dev. *13*, 76–86.

Jacobs, T., Graefe, S.E., Niknafs, S., Gaworski, I., and Fleischer, B. (2002). Murine malaria is exacerbated by CTLA-4 blockade. J. Immunol. *169*, 2323–2329.

Kensler, T.W., Wakabayashi, N., and Biswal, S. (2007). Cell survival responses to environmental stresses via the Keap1-Nrf2-ARE pathway. Annu. Rev. Pharmacol. Toxicol. *47*, 89–116.

Larsen, R., Gozzelino, R., Jeney, V., Tokaji, L., Bozza, F.A., Japiassú, A.M., Bonaparte, D., Cavalcante, M.M., Chora, A., Ferreira, A., et al. (2010). A central

role for free heme in the pathogenesis of severe sepsis. Sci. Transl. Med. *2*, 51ra71.

McDaid, J., Yamashita, K., Chora, A., Ollinger, R., Strom, T.B., Li, X.C., Bach, F.H., and Soares, M.P. (2005). Heme oxygenase-1 modulates the allo-immune response by promoting activation-induced cell death of T cells. FASEB J. *19*, 458–460.

Medzhitov, R., Schneider, D.S., and Soares, M.P. (2012). Disease tolerance as a defense strategy. Science *335*, 936–941.

Miller, L.H., Ackerman, H.C., Su, X.Z., and Wellems, T.E. (2013). Malaria biology and disease pathogenesis: insights for new treatments. Nat. Med. *19*, 156–167.

Mishra, S.K., and Newton, C.R. (2009). Diagnosis and management of the neurological complications of falciparum malaria. Nat Rev Neurol *5*, 189–198.

Miu, J., Mitchell, A.J., Müller, M., Carter, S.L., Manders, P.M., McQuillan, J.A., Saunders, B.M., Ball, H.J., Lu, B., Campbell, I.L., and Hunt, N.H. (2008). Chemokine gene expression during fatal murine cerebral malaria and protection due to CXCR3 deficiency. J. Immunol. *180*, 1217–1230.

Motterlini, R., Foresti, R., Intaglietta, M., and Winslow, R.M. (1996). NO-mediated activation of heme oxygenase: endogenous cytoprotection against oxidative stress to endothelium. Am. J. Physiol. *270*, H107–H114.

Mustafa, A.K., Gadalla, M.M., and Snyder, S.H. (2009). Signaling by gasotransmitters. Sci. Signal. *2*, re2.

Naughton, P., Hoque, M., Green, C.J., Foresti, R., and Motterlini, R. (2002). Interaction of heme with nitroxyl or nitric oxide amplifies heme oxygenase-1 induction: involvement of the transcription factor Nrf2. Cell. Mol. Biol. (Noisy-le-grand) *48*, 885–894.

Nitcheu, J., Bonduelle, O., Combadiere, C., Tefit, M., Seilhean, D., Mazier, D., and Combadiere, B. (2003). Perforin-dependent brain-infiltrating cytotoxic CD8+ T lymphocytes mediate experimental cerebral malaria pathogenesis. J. Immunol. *170*, 2221–2228.

Ong, P.K., Melchior, B., Martins, Y.C., Hofer, A., Orjuela-Sánchez, P., Cabrales, P., Zanini, G.M., Frangos, J.A., and Carvalho, L.J. (2013). Nitric oxide synthase dysfunction contributes to impaired cerebroarteriolar reactivity in experimental cerebral malaria. PLoS Pathog. *9*, e1003444.

Pamplona, A., Ferreira, A., Balla, J., Jeney, V., Balla, G., Epiphanio, S., Chora, A., Rodrigues, C.D., Gregoire, I.P., Cunha-Rodrigues, M., et al. (2007). Heme oxygenase-1 and carbon monoxide suppress the pathogenesis of experimental cerebral malaria. Nat. Med. *13*, 703–710.

Patel, R.P., and Gladwin, M.T. (2004). Physiologic, pathologic and therapeutic implications for hemoglobin interactions with nitric oxide. Free Radic. Biol. Med. *36*, 399–401.

Rother, R.P., Bell, L., Hillmen, P., and Gladwin, M.T. (2005). The clinical sequelae of intravascular hemolysis and extracellular plasma hemoglobin: a novel mechanism of human disease. JAMA *293*, 1653–1662.

Sato, K., Balla, J., Otterbein, L., Smith, R.N., Brouard, S., Lin, Y., Csizmadia, E., Sevigny, J., Robson, S.C., Vercellotti, G., et al. (2001). Carbon monoxide generated by heme oxygenase-1 suppresses the rejection of mouse-to-rat cardiac transplants. J. Immunol. *166*, 4185–4194.

Schneider, D.S. (2011). Tracing personalized health curves during infections. PLoS Biol. *9*, e1001158.

Schneider, D.S., and Ayres, J.S. (2008). Two ways to survive infection: what resistance and tolerance can teach us about treating infectious diseases. Nat. Rev. Immunol. *8*, 889–895.

Seixas, E., Gozzelino, R., Chora, A., Ferreira, A., Silva, G., Larsen, R., Rebelo, S., Penido, C., Smith, N.R., Coutinho, A., and Soares, M.P. (2009). Heme oxygenase-1 affords protection against noncerebral forms of severe malaria. Proc. Natl. Acad. Sci. USA *106*, 15837–15842.

Silva, G., Jeney, V., Chora, A., Larsen, R., Balla, J., and Soares, M.P. (2009). Oxidized hemoglobin is an endogenous proinflammatory agonist that targets vascular endothelial cells. J. Biol. Chem. *284*, 29582–29595.

Soares, M.P., Marguti, I., Cunha, A., and Larsen, R. (2009). Immunoregulatory effects of HO-1: how does it work? Curr. Opin. Pharmacol. *9*, 482–489.

Spaccapelo, R., Janse, C.J., Caterbi, S., Franke-Fayard, B., Bonilla, J.A., Syphard, L.M., Di Cristina, M., Dottorini, T., Savarino, A., Cassone, A., et al. (2010). Plasmepsin 4-deficient *Plasmodium berghei* are virulence attenuated and induce protective immunity against experimental malaria. Am. J. Pathol. *176*, 205–217.

Suzuki, T., Motohashi, H., and Yamamoto, M. (2013). Toward clinical application of the Keap1-Nrf2 pathway. Trends Pharmacol. Sci. *34*, 340–346.

Taylor, T.E., Fu, W.J., Carr, R.A., Whitten, R.O., Mueller, J.S., Fosiko, N.G., Lewallen, S., Liomba, N.G., and Molyneux, M.E. (2004). Differentiating the pathologies of cerebral malaria by postmortem parasite counts. Nat. Med. *10*, 143–145.

Tenhunen, R., Marver, H.S., and Schmid, R. (1968). The enzymatic conversion of heme to bilirubin by microsomal heme oxygenase. Proc. Natl. Acad. Sci. USA *61*, 748–755.

Trovoada, Mde.J., Martins, M., Ben Mansour, R., Sambo, Mdo.R., Fernandes, A.B., Antunes Gonçalves, L., Borja, A., Moya, R., Almeida, P., Costa, J., et al. (2014). NOS2 variants reveal a dual genetic control of nitric oxide levels, susceptibility to *Plasmodium* infection, and cerebral malaria. Infect. Immun. *82*, 1287–1295.

Villegas-Mendez, A., Greig, R., Shaw, T.N., de Souza, J.B., Gwyer Findlay, E., Stumhofer, J.S., Hafalla, J.C., Blount, D.G., Hunter, C.A., Riley, E.M., and Couper, K.N. (2012). IFN-γ-producing CD4+ T cells promote experimental cerebral malaria by modulating CD8+ T cell accumulation within the brain. J. Immunol. *189*, 968–979.

Walther, M., De Caul, A., Aka, P., Njie, M., Amambua-Ngwa, A., Walther, B., Predazzi, I.M., Cunnington, A., Deininger, S., Takem, E.N., et al. (2012). HMOX1 gene promoter alleles and high HO-1 levels are associated with severe malaria in Gambian children. PLoS Pathog. *8*, e1002579.

Weiss, G., Werner-Felmayer, G., Werner, E.R., Grünewald, K., Wachter, H., and Hentze, M.W. (1994). Iron regulates nitric oxide synthase activity by controlling nuclear transcription. J. Exp. Med. *180*, 969–976.

Weiss, G., Thuma, P.E., Biemba, G., Mabeza, G., Werner, E.R., and Gordeuk, V.R. (1998). Cerebrospinal fluid levels of biopterin, nitric oxide metabolites, and immune activation markers and the clinical course of human cerebral malaria. J. Infect. Dis. *177*, 1064–1068.

Yeo, T.W., Lampah, D.A., Rooslamiati, I., Gitawati, R., Tjitra, E., Kenangalem, E., Price, R.N., Duffull, S.B., and Anstey, N.M. (2013). A randomized pilot study of L-arginine infusion in severe falciparum malaria: preliminary safety, efficacy and pharmacokinetics. PLoS ONE *8*, e69587.